THE JOURNAL OF PHYSICAL CHEMISTRY C

Article

pubs.acs.org/JPCC

Time Evolution of a Cl-Terminated Si Surface at Ambient Conditions

P. Chatterjee and S. Hazra*

Saha Institute of Nuclear Physics, 1/AF Bidhannagar, Kolkata 700064, India

ABSTRACT: The stability of Cl-terminated Si surface at ambient conditions and its evolution with time, which have immense importance for the growth of interesting nanostructures on it, were investigated using complementary methods. Wetting of water, i.e., contact angle measurements, which provide macroscopic level information, shows transition in the nature of Cl−Si surface from weak-hydrophilic toward weak-hydrophobic with time. Electron density profiles, obtained from X-ray reflectivity (XR) measurements, suggest that such a transition is associated with the growth of less uniform oxide layer. Structures of CTAB−silica mesostructured films on as-prepared and time-evolved Cl−Si substrates, obtained from XR and grazing incidence small-angle X-ray scattering measurements, show transition from strongly attached near circular micelles to weakly attached more elliptical micelles, confirming the transition (from weak-hydrophilic toward weak-hydrophobic) in microscopic level and growth of less homogeneous oxide layer. The critical time of such a transition is about 50 h, which actually represents the stability or the critical time of Cl desorption and oxide growth of the Cl−Si surface at ambient conditions.

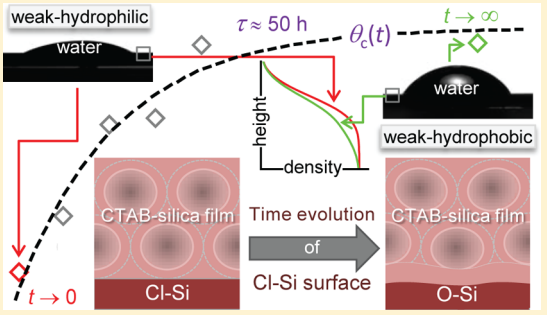

INTRODUCTION

Passivation of semiconductor surface, especially silicon surface, is extremely important for their applications in a wide range of fields, including nanotechnology, microelectronics, optoelectronics, biomedical, and biological sensors.[1,2] Passivation or termination of Si surface by different atoms or groups like, −OH, −H, −Cl, −Br, etc., essentially prevents contamination and surface defect states, thus controlling the electronic properties of the surface or interface.[2] It also tunes the surface free energy, polar−nonpolar (hydrophilic−hydrophobic) or electrostatic nature, and the reactivity of the surface.[3−8] Such nature of the passivated surface and its stability plays an important role in the growth of interesting nanostructures on it[5,6,9−15] and thus becomes one of the thrust area of investigation.

Among different passivated surfaces, Cl-terminated Si surface, which has good Si−Cl bond stability and can be prepared easily through the wet-chemical process,[16−18] is drawing tremendous attention due to its higher reactivity compared to the H-terminated Si surface for the functionalization reactions.[19,20] Understanding the nature (hydrophilic−hydrophobic) of the Cl−Si surface and its stability is very important for its proper utilization. The nature of a surface is well evident from the growth of amphiphilic molecules[5,15,21−23] or composite materials[7,8] having both hydrophilic and hydrophobic parts, apart from conventional contact angle (CA) or water adhesion measurements.[24−26] Recently, weak-hydrophilic[26] or hydrophilic-like nature of the Cl−Si surface, in the molecular level, is determined from the structures of the deposited CTAB−silica 2D-hexagonal mesostructured films on it,[8] thus removing contradictory or incomplete information about the nature of the surface.[27,28]

The stability of the Cl−Si surface, on the other hand, is less studied.[18,29] It is known that the stability of a passivated surface depends on the environments, namely humidity of air, oxygen content in air, dissolved oxygen in water, and metal impurity on the surface.[13,14,18,21,22,29] Native oxide is normally grown on the Si surface desorbing the passivated atoms. Thus, understanding the growth of oxide layer is one way to understand the stability−instability of a passivated surface. Soft X-ray photoelectron spectroscopy (SXPS)[18] and high-resolution electron energy loss spectroscopy (HREELS)[29] were used to identify the presence of silicon oxide on the surface and its growth with time. Oxidation can change the chemical nature and/or the roughness of the surface, which in turn can change the hydrophilic−hydrophobic nature of the surface. However, not much work is carried out to understand the stability−instability information on the Cl−Si surface, from the point of view of hydrophilic−hydrophobic nature of the surface. Simple CA measurements along with the X-ray scattering measurements can monitor not only the hydrophilic−hydrophobic nature of the surface but also its quantitative evolution, i.e., its stability, which is never estimated before.

Here the evolution of the Cl−Si surface with time in ambient conditions is monitored directly using CA and X-ray reflectivity (XR) techniques.[5,13,30−32] The structures of the CTAB−silica 2D-hexagonal mesostructured films[33−35] deposited at different point of time were estimated by the complementary XR and grazing incidence small-angle X-ray scattering (GISAXS)[8,36−40] techniques and were used to understand the evolution of the

Received: February 11, 2014
Revised: May 2, 2014
Published: May 6, 2014

Cl−Si surface. Transition from weak-hydrophilic toward weak-hydrophobic is clearly evident with time. The characteristic transition time is estimated, and the possible reasons for such transition are discussed.

EXPERIMENT

Preparation. Cl-terminated Si surfaces were prepared as reported before.[8] In short, after removing the organic contaminants,[13] Si(111) substrates (of size 15 × 15 mm^2) were treated with the RCA cleaning method, where the substrates were boiled at 100 °C for about 10 min in a mixed solution of ammonium hydroxide [NH_4OH, Merck, 30%], hydrogen peroxide [H_2O_2, Merck, 30%], and Milli-Q water (NH_4OH:H_2O_2:H_2O = 1:1:5, by volume).[3−5,7] Further etchings in a solution of hydrogen fluoride [HF, Merck, 10%] for 30 s and then in a solution of ammonium fluoride [NH_4F, Merck, 40%] for 2 min at room temperature (25 °C)[4] were carried out to get H-terminated Si substrates. The H−Si substrates were then chlorinated through wet-chemical method as reported in the literature.[16] A stock chlorinating solution was prepared by dissolving phosphorus pentachloride [PCl_5, Merck] in chlorobenzene [C_6H_5Cl, Merck] to form a near-saturated solution (typically 0.6 M). The solution was heated at ∼60 °C for 1 h for complete dissolution of the PCl_5. Immediately before use, few grains of benzoyl peroxide (∼300 mg) were added to the stock solution (∼80 mL). The H−Si samples were immersed into the solution and heated to 90−100 °C for 45 min. The samples were then rinsed with anhydrous tetrahydrofuran and anhydrous methanol to get Cl-terminated Si substrates. Cl−Si samples were kept at ambient conditions [with constant temperature ∼25 °C and relative humidity ∼40%] for different durations to understand the stability.

A silica−surfactant solution was prepared by two-step synthesis method using tetraethyl orthosilicate [TEOS, Si-$(OC_2H_5)_4$, Sigma-Aldrich, 99.999%], cetyltrimethylammonium bromide [CTAB, $C_{16}H_{33}N(CH_3)_3Br$, Fluka, ≥99%], ethanol [C_2H_5OH, Merck, absolute], Milli-Q water (resistivity 18.2 MΩ cm), and hydrochloric acid [HCl, Merck, 35%] as reported before.[7,8] In the first step, a silica sol was prepared with TEOS in acidic condition with molar ratio of TEOS:C_2H_5OH:H_2O = 1:4.5:1 and finally added the required amount of HCl to the solution to keep the pH ≈ 1. The solution was then stirred for 1 h at room temperature. In parallel, a second solution was prepared by dissolving 0.348 g of CTAB in ethanol and water of molar ratio 3.66:1. Finally, the second solution was added to the first one to get the final solution in the molar ratio of TEOS:CTAB:C_2H_5OH:H_2O = 1:0.19:20:5.5, which was then stirred for another 1 h and aged for 2 h. The solution was diluted by adding excess ethanol (of amount 35 cm^3) to the stock solution, and the films were prepared from that solution (at temperature 25−30 °C and relative humidity 70−75%) using a spin-coater (EC101, Headway Research) at a speed of 4000 rpm on different time-evolved Cl−Si substrates. Time-evolved substrate is referred as *N*d, where *N* indicates the time (in days) for which it is kept at ambient conditions. For as-prepared substrate $N = 0$.

Characterization. CA measurements of a Cl−Si sample were carried out just after preparation and subsequently in different days, using a CA goniometer (ramé-hart), to investigate the evolution of the hydrophilic−hydrophobic nature of the surface with time. For the measurement, a drop (5 μL) of water (Milli-Q) was placed on the sample surface. Each day, the CA values were noted for five successive times at an interval of 20 s. Such measurements were done at more than five different regions over the sample surface. The CA value was determined by taking the average of the final measurements at the five different regions. It can be noted that here we have not measured the advancing and receding contact angles, as mentioned before,[8] which are more appropriate. What we measured is the so-called as-placed CA, whose changes are qualitatively similar to those of the equilibrium CA.[25]

XR measurements of a Cl−Si sample were performed just after preparation (within a day) and subsequently in different days, using a versatile X-ray diffractometer (VXRD) setup.[41] XR measurements of the as-prepared and dried CTAB−silica mesostructured films on different time-evolved Cl−Si substrates were also carried out using VXRD setup. VXRD consists of a diffractometer (D8 Discover, Bruker AXS) with Cu source (sealed tube) followed by a Göbel mirror to select and enhance Cu Kα radiation (λ = 1.54 Å). The diffractometer has a two-circle goniometer [$\theta(\omega) - 2\theta$] with quarter-circle Eulerian cradle as sample stage. The latter has two circular (χ and ϕ) and three translational (X, Y, and Z) motions. Scattered beam was detected using NaI scintillation (point) detector. Data were taken in the specular condition; i.e., incident angle, α is equal to the reflected angle, β ($\alpha = \beta = \theta$). Under such condition there exists a nonvanishing wave vector component, q_z, which is equal to $(4\pi/\lambda)$ sin θ with resolution 0.002 $Å^{-1}$. XR data essentially provide an electron-density profile (EDP), i.e., in-plane ($x - y$) average electron density (ρ) as a function of depth (z) in high resolution,[42] from which one can estimate the roughness of Cl−Si substrate, thickness, and coverage of oxide layer on it, if any. Also, one can estimate the nature of the film−substrate interface, thickness, interlayer separation, and the average density or porosity of the mesostructured films.[7]

On the other hand, GISAXS measurements of the dried CTAB−silica mesostructured films on different time-evolved Cl−Si substrates were performed using synchrotron source (MiNaXS beamline, PETRA III) at energy 11.4 keV.[43] The scattered beam was detected using 2D detector (PILATUS 1M, Dectris, having 981 × 1043 pixels and 172 μm pixel size) by placing it about 171 cm apart from the sample. For data collection, incident angle, α was kept (0.25°) slightly greater than the critical angle, α_c, of the sample. The direct beam was stopped, and the specular reflected beam was attenuated by two separate point-like beam stops to avoid the saturation of the detector. GISAXS data provides the in-plane and out-of-plane separations in a mesostructured film, from which one can extract the unit cell parameters and the shape of the silica coated micelles.[7]

RESULTS AND DISCUSSION

Evolution from Wetting−Dewetting of Water. The hydrophilic−hydrophobic nature of a surface and its evolution with time, in the macroscopic level, can be easily estimated from the wetting−dewetting of water, i.e., from the CA measurements. Typical images of water drops on a time-evolved Cl−Si substrate are shown in Figure 1. Dewetting with time is clearly evident from these images. Corresponding average value of CA (θ_c) with error bar are plotted as a function of time (t) in Figure 2. The value of θ_c increases with time, which is initially fast then saturates with time. Such variation of θ_c can be expressed quantitatively using standard exponential dependence:

dx.doi.org/10.1021/jp501480x | J. Phys. Chem. C 2014, 118, 11350−11356

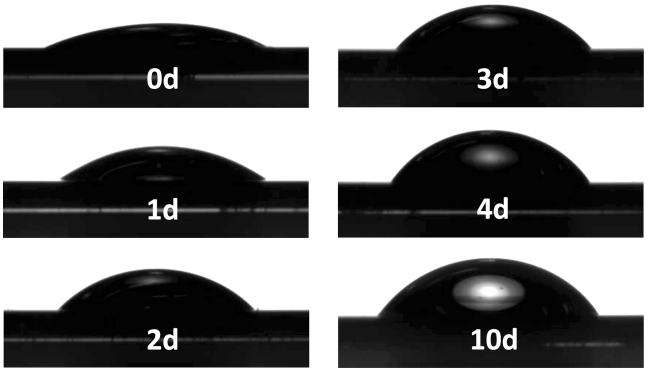

Figure 1. Typical images of water drops on a time-evolved Cl−Si substrate. *N*d indicates the substrate that is evolved for *N* days at ambient conditions.

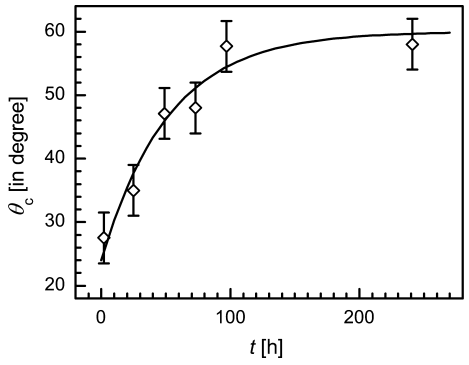

Figure 2. Variation of contact angle (θ_c) of Cl−Si surface with time at ambient conditions. Symbols are the experimental data, and the solid line through the data is the analyzed curve.

$$\theta_c = \theta_{c0} + \Delta\theta_c(1 - e^{-t/\tau}) \quad (1)$$

where θ_{c0} is the CA of the Cl−Si surface at $t = 0$, $\Delta\theta_c$ is the maximum change in the CA with time at ambient condition, i.e., the CA of the Cl−Si surface at $t \rightarrow \infty$ is $\theta_{c\infty} = \theta_{c0} + \Delta\theta_c$, and τ is the critical transition time. The variation of θ_c has been fitted using eq 1, and the fitted profile is shown in Figure 2. The parameters obtained from the fitting are $\theta_{c0} \approx 24°$, $\theta_{c\infty} \approx 60°$, and $\tau \approx 50$ h. Although there are diversity in the definitions of hydrophilic and hydrophobic surfaces, a recent review article[26] proposed different measures and classifications of the hydrophilic−hydrophobic nature of solid surfaces based on different parameters such as the contact angle, the water adhesion tension, the work of spreading, or the energy of hydration. Accordingly, $0 < \theta_c < 56°–65°$ is termed as weak-hydrophilic and $56°–65° < \theta_c < 90°$ is termed as weak-hydrophobic surfaces. Following this classification, the transition in the nature of the Cl−Si surface at ambient conditions is from weak-hydrophilic toward weak-hydrophobic, and the critical time for such transition is about 50 h.

Evolution from Electron Density Profile of Substrate. XR data (R) normalized with Fresnel's reflectivity (R_F) for a time-evolved Cl−Si substrate are shown in Figure 3. A dip is present in all the apparently featureless curves. The dip becomes sharper and its position shifted toward the left with time, indicating probable increase in the roughness of the substrate surface. To have a better idea about the nature of the substrate surface, the XR data have been analyzed using Parratt's formalism.[44] For the analysis, a layer on the top of the

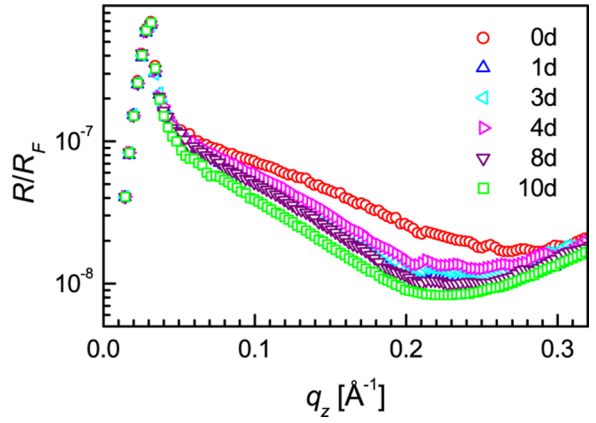

Figure 3. Normalized XR data of a time-evolved Cl−Si substrate. *N*d indicates the substrate that is evolved for *N* days at ambient conditions.

substrate is assumed. Considering roughness (σ), layer thickness (d_{ox}), and electron density (ρ) as parameters, the XR data have been analyzed. Best fitted curves along with the XR data for the Cl−Si substrate measured initially (0d) and after 10 days (10d) are shown in Figure 4. Corresponding

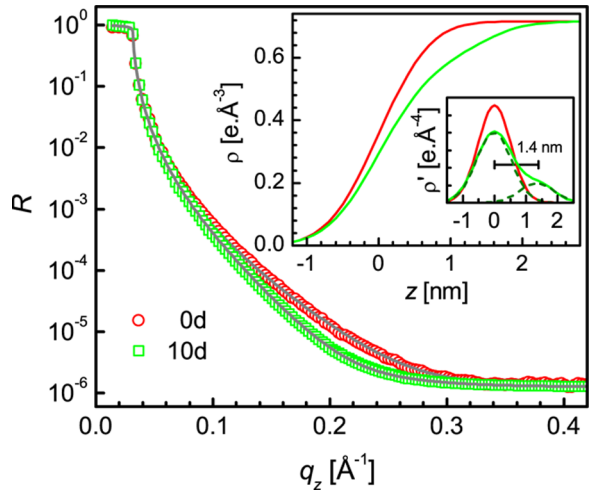

Figure 4. XR data (different symbols) and analyzed curves (solid line) of Cl−Si substrate measured initially (as-prepared) and finally (after evolved at ambient conditions for 10 days). Inset: corresponding EDPs and their derivatives.

EDPs and their derivatives are shown in the insets of Figure 4. Decrease in the value of ρ on the top part of the substrate with time is evident from the EDPs. Such low density layer corresponds to the oxide layer. The values of σ (about 0.54 and 0.56 nm) and d_{ox} (about 0 and 1.4 nm), estimated from the derivatives of the EDPs (0d and 10d), suggest no appreciable increase in the roughness with time but growth of oxide layer on Cl−Si substrate.

Evolution from Structure of Deposited Film. *Interface and Out-of-Plane Structures from XR.* XR data of the as-prepared CTAB−silica mesostructured films on different time-evolved Cl−Si substrates are shown in Figure 5. Two strong pseudo-Bragg peaks are visible in all the curves, which correspond to the first and second orders of the (02) Bragg peak for the 2D-hexagonal mesostructure,[35] suggesting the formation of well-ordered compressed 2D-hexagonal structure,[7]

dx.doi.org/10.1021/jp501480x | J. Phys. Chem. C 2014, 118, 11350−11356

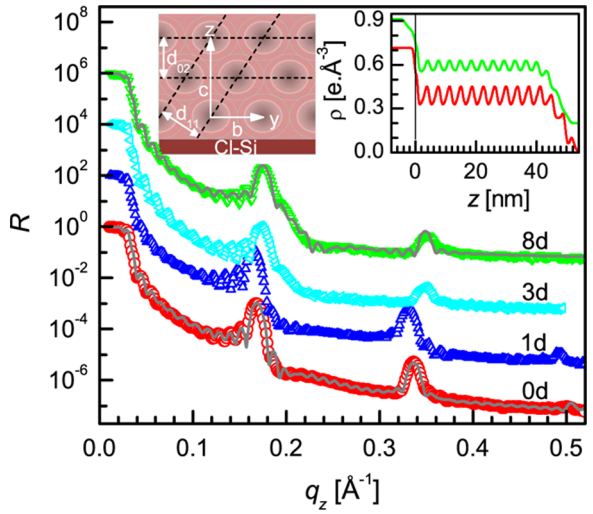

Figure 5. XR data (different symbols) and analyzed curves (solid line) of the as-prepared CTAB−silica mesostructured thin films on different time-evolved Cl−Si substrates (curves are shifted vertically for clarity). *N*d indicates the substrate that is evolved for *N* days at ambient conditions. Insets: schematic of a compressed 2D-hexagonal structure showing unit cell parameters (*b* and *c*) and lattice spacings (d_{02} and d_{11}) for an equivalent centered rectangular (*c*2*mm*) unit and analyzed EDPs of the films on initial (as-prepared) and finally evolved (after 8 days) substrates.

as shown schematically in the inset of Figure 5. Kiessig fringes, which are the measure of the total film thickness, are very clearly visible for all the XR profiles before first Bragg peak. The nature of the fall of XR profile after the first Bragg peak is found different for the different films. The fall, which is sharp for the film on 0d substrate, became gradual for the film on 8d substrate. This may be due to the change in the film−substrate interface. The values of c_i (i.e., $2d_{02}$) obtained from the (02) Bragg peak positions for the as-prepared films on 0d and 8d substrates are tabulated in Table 1 with an accuracy better than

Table 1. In-Plane (*b*) and Out-of-Plane (*c*) Unit Cell Parameters of the Compressed 2D-Hexagonal Structure and the Ratio of Semimajor and Semiminor Axis (r_l/r_s) Corresponding to the Equivalent Ellipse for the Films on As-Prepared (0d) and Time-Evolved (8d) Cl−Si Substrates Obtained from XR and GISAXS Measurements[a]

substrate	c_i (nm)	c_f (nm)	b_f (nm)	$(r_l/r_s)_i$	$(r_l/r_s)_f$
0d	7.48	7.28	5.3	1.22	1.25
8d	7.16	7.06	5.1	1.23 (1.28)	1.25

[a]Subscripts *i* and *f* represent parameters corresponding to the film at initial and final stages of measurements, i.e., for the as-prepared and dried film, respectively.

±0.02 nm. Small change in the value of c_i is observed, which may be related to the change in the shape of the micelles due to the change in the interface. Similarly, the intensity of the first- and second-order Bragg peaks for the film on 8d substrate are about 5 and 12 times less compared to the peaks for the film on 0d substrate, indicating deterioration in the ordering, probably due to the change in the interface.

To get further information about the structure of the films, especially about the film−substrate interface, the XR data have been analyzed considering a model oscillatory EDP, arising from periodic repetitions of two stacked layers as considered before.[7] One layer is made of cylindrical surfactant aggregates plus a silica wall, and another layer is made of silica only (as shown schematically in the inset of Figure 5), having different averaged electron density, thickness, and roughness. In addition, special attention is paid to the initial layer through which the film is attached with the substrate, as it decides the nature of the substrate surface. Based on this model, the best fit XR profiles for the films on 0d an 8d substrates are shown in Figure 5 along with the corresponding EDPs in the inset. Similar to the bare substrate, the growth of oxide layer (i.e., decrease in the value of ρ) on the top part of the substrate with time is evident from the EDPs. Small decrease in the value of d_{02} and in the contrast between two consecutive layers are also observed for the film, which may be related to the change in the shape of the micelles from nearly circular to more elliptical, change in the film−substrate attachment from strong to weak, and deterioration in the ordering.

In-Plane and Out-of-Plane Structures from GISAXS. GISAXS patterns of the dried CTAB−silica mesostructured films on different time-evolved Cl−Si substrates are shown in Figure 6. (02) and (11) Bragg spots, signatures of a compressed

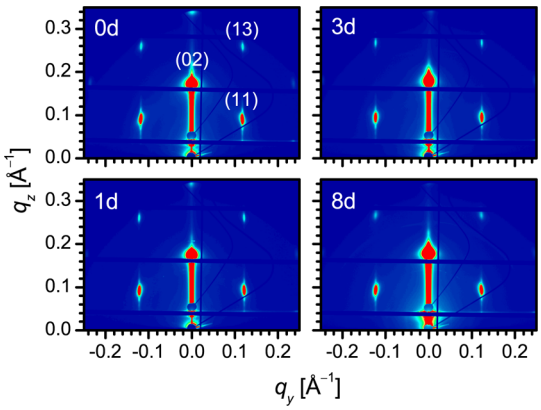

Figure 6. GISAXS patterns of the dried CTAB−silica mesostructured thin films on different time-evolved Cl−Si substrates, showing (02), (11), and (13) Bragg spots of the compressed 2D-hexagonal structure. *N*d indicates the substrate that is evolved for *N* days at ambient conditions.

2D-hexagonal structure, are evident in all the patterns. Weak (13) Bragg spot is also evident in all the patterns. To have better idea about the positions of the spots, line profiles along q_z and q_y directions and through the (02) and (11) Bragg spots for the films on 0d and 8d substrates are plotted in Figures 7 and 8, respectively. The change in the position of peaks for the two films are clearly evident. The values of c_f and b_f, obtained from the peaks with an accuracy better than ±0.02 nm, are tabulated in Table 1. The decrease in the value of c_f is observed similar to c_i, but the change is small. The decrease in the value of b_f is also observed, unlike our previous studies,[7,8] which is interesting to note. Considering $b_i = b_f$, the ratio of semimajor and semiminor axis (r_l/r_s) of equivalent ellipse is estimated from $\sqrt{3}/(c/b)$ and is listed in Table 1. The values of r_l/r_s for the dried films on both the substrates are found same, while that for the as-prepared films on 8d substrate is found slightly large compared to that on 0d substrate. It can be noted that we have assumed $b_i = b_f$. This is a valid assumption if the film−substrate interaction is strong, as expected for the film on 0d substrate. However, if the film−substrate interaction is weak, which may be a possibility for the film on 8d substrate, then b_i

dx.doi.org/10.1021/jp501480x | J. Phys. Chem. C 2014, 118, 11350−11356

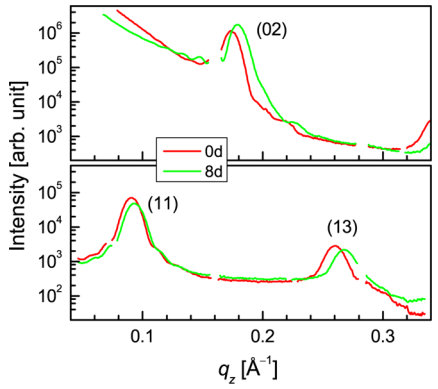

Figure 7. GISAXS line profiles along q_z direction and through (02) and (11) Bragg spots for the dried CTAB–silica mesostructured thin films on as-prepared and 8 day-evolved Cl–Si substrates.

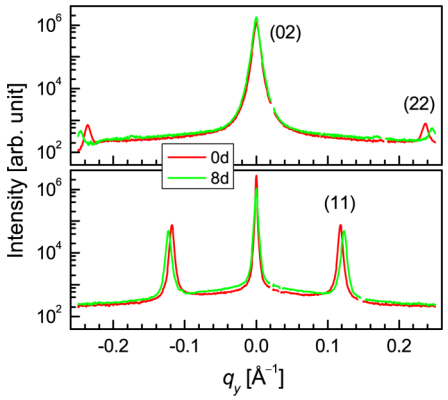

Figure 8. GISAXS line profiles along q_y direction and through (02) and (11) Bragg spots for the dried CTAB–silica mesostructured thin films on as-prepared and 8 day-evolved Cl–Si substrates.

can be greater than b_f. Considering same b_i value (5.3 nm) for both the as-prepared films, the value of $(r_l/r_s)_i$ for the film on 8d substrate is recalculated and shown in parentheses in Table 1. This confirms that the micelles are less elliptical (i.e., more circular) on the 0d substrate and more elliptical on the 8d substrate during the initial stages of the film formation, as predicted from the XR data analysis. Further with time, the shapes of the micelles on both the substrates become almost the same. This also indicates that the attachment of the film on the 0d substrate is strong, while that on the 8d substrate is weak.

Time Evolution of Cl–Si and Proposed Mechanism. The evolution of Cl–Si surface with time at ambient conditions, obtained from different measurements, is shown schematically in Figure 9. Evolution in the nature of surface from weak-hydrophilic toward weak-hydrophobic, in macroscopic scale, is evident from the change in the wetting–dewetting properties of water. It is well-known from SXPS[18] and HREELS[29] studies that at ambient conditions oxide grows on the Si surface desorbing the Cl from the Cl–Si surface. EDPs of bare substrate obtained from the XR measurements support the growth of oxide layer, the roughness of which is found slightly large, probably due to the inhomogeneous growth of oxide layer with time. Structures of the CTAB–silica mesostructured films show transition from strongly attached near circular micelles to weakly attached more elliptical micelles, suggesting similar transition of Cl–Si surface from

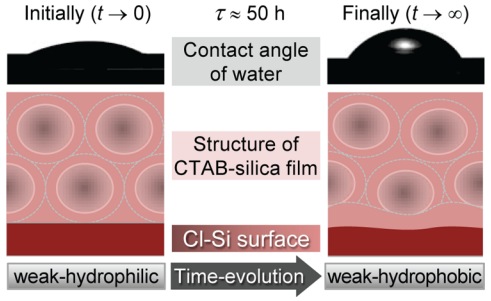

Figure 9. Schematic of the wetting–dewetting of water (in mm length scale) and the structures of the CTAB–silica films (in nm length scale) on as-prepared and time-evolved Cl–Si surfaces as predicted from the CA, XR, and GISAXS measurements, suggesting weak-hydrophilic (Cl–Si) to more toward weak-hydrophobic (O–Si) transition with time and providing characteristic transition or stability time (τ).

weak-hydrophilic toward weak-hydrophobic with time even in microscopic level. The hydrophilic–hydrophobic nature of a surface can arise from its chemical (such as Cl, O, etc.) and/or structural (such as low or high height fluctuation or roughness) natures. Here negligible change in the roughness is observed, suggesting that the variation of θ_c with time is mainly due to the growth of oxides on the Cl–Si surface, similar to that indicated for other passivated-Si surface.[5,13] Also, the exponential decay term corresponds to the desorption of Cl from the Cl–Si surface, similar to that indicated for the Br–Si surface from X-ray standing wave studies.[45] Thus, the critical time of transition, which is found to be about 50 h, essentially represents the critical oxide growth time or the critical stability–instability time of the Cl–Si surface at ambient conditions.

The evolution of hydrophilic–hydrophobic nature of the Cl–Si surface at ambient conditions can be well realized considering its polar–nonpolar nature. The relatively strong electronegativity difference between Cl and Si (1.26)[46] makes the as-prepared Cl–Si surface relatively polar and weak-hydrophilic.[8] Similarly, the electronegativity difference between O and Si (1.54) is quite high,[46] but each O atom is connected to two Si atoms, which makes the effective electronegativity difference quite low. Such relatively low electronegativity difference is probably responsible for the relatively nonpolar and more toward weak-hydrophobic nature of the oxide grown Si surface. Accordingly, relatively wetting and dewetting natures of water are found in as-prepared Cl–Si and oxide grown Si surfaces. Further, silica-coated cylindrical micelles of near circular shape are adsorbed through their silica parts onto this homogeneous and weak-hydrophilic Cl–Si surface to form well-ordered structure. The attachment of the film to the Cl–Si surface is quite strong, which creates strong asymmetric stress on the micelles while drying, especially near the substrate. On the other hand, hemicylindrical micelles or cylindrical micelles of elliptical shape are attached onto the oxide-grown Si surface, which is more toward weak-hydrophobic and less homogeneous to form less ordered structure. The attachment of the film to the oxide-grown Si surface is quite weak, which tries to release the stress of the micelles while drying.

■ CONCLUSIONS

The stability–instability of a Cl-terminated Si surface, prepared by wet chemical process, was examined using different parameters. Initially low (~24°) CA value of the as-prepared Cl–Si surface finally becomes relatively high (~60°) when kept

dx.doi.org/10.1021/jp501480x | J. Phys. Chem. C 2014, 118, 11350–11356

at ambient conditions for a sufficient time. This indicates transition in the nature of surface from weak-hydrophilic toward weak-hydrophobic with time. Electron density profiles suggest that such transition is mainly associated with the growth of oxide layer. That means Cl−Si becomes O−Si. However, oxide growth with time is not homogeneous or uniform. Structures of CTAB−silica mesostructured films on as-prepared and time-evolved Cl−Si substrates indicate that silica-coated cylindrical micelles of near circular shape are adsorbed through their silica parts onto the homogeneous and weak-hydrophilic Cl−Si surface to form well-ordered structure, while hemicylindrical micelles or cylindrical micelles of elliptical shape are attached onto the oxide-grown Si surface which is less homogeneous and more toward weak-hydrophobic to form less ordered structure. The attachment of the film to the Cl−Si surface is quite strong, while to the oxide-grown Si surface is quite weak. Accordingly, previous one creates strong asymmetric stress on the micelles and latter on tries to release the stress of the micelles, while drying. Transition from weak-hydrophilic toward weak-hydrophobic of the Cl−Si surface also provides the critical transition time ($\tau \approx 50$ h), which is a measure of its stability and critical oxide growth time at ambient conditions. The quantitative information on the stability of the Cl−Si surface, which was not available before, is of immense importance for the growth of interesting nanostructures on it.

AUTHOR INFORMATION

Corresponding Author

*E-mail: satyajit.hazra@saha.ac.in (S.H.).

Notes

The authors declare no competing financial interest.

ACKNOWLEDGMENTS

The authors thank Prof. N. R. Ray and Dr. S. Roth for their support in contact angle and GISAXS measurements, respectively. The financial support received from Saha Institute of Nuclear Physics under DST-DESY project to carry out GISAXS experiments at PETRA III is thankfully acknowledged.

REFERENCES

(1) Buriak, J. M. Organometallic Chemistry on Silicon and Germanium Surfaces. *Chem. Rev.* **2002**, *102*, 1271−1308.
(2) Derycke, V.; Soukiassian, P. G.; Amy, F.; Chabal, Y. J.; Dangelo, M. D.; Enriquez, H. B.; Silly, M. G. Nanochemistry at the Atomic Scale Revealed in Hydrogen-Induced Semiconductor Surface Metallization. *Nat. Mater.* **2003**, *2*, 253−258.
(3) Okorn-Schmidt, H. F. Characterization of Silicon Surface Preparation Processes for Advanced Gate Dielectrics. *IBM J. Res. Dev.* **1999**, *43*, 351−366.
(4) Zhang, X. G. *Electrochemistry of Silicon and its Oxide*; Kluwer Academic: New York, 2004.
(5) Bal, J. K.; Kundu, S.; Hazra, S. Growth and Stability of Langmuir-Blodgett Films on OH-, H-, or Br-Terminated Si(001). *Phys. Rev. B* **2010**, *81*, 045404.
(6) Dan, Y.; Seo, K.; Takei, K.; Meza, J. H.; Javey, A.; Crozier, K. B. Dramatic Reduction of Surface Recombination by in Situ Surface Passivation of Silicon Nanowires. *Nano Lett.* **2011**, *11*, 2527−2532.
(7) Chatterjee, P.; Hazra, S.; Amenitsch, H. Substrate and Drying Effect in Shape and Ordering of Micelles Inside CTAB-Silica Mesostructured Films. *Soft Matter* **2012**, *8*, 2956−2964.
(8) Chatterjee, P.; Hazra, S. The Hydrophilic/Hydrophobic Nature of a Cl-Terminated Si Surface. *Soft Matter* **2013**, *9*, 9799−9806.
(9) Zasadzinski, J.; Viswanathan, R.; Madsen, L.; Garnaes, J.; Schwartz, D. Langmuir-Blodgett Films. *Science* **1994**, *263*, 1726−1733.
(10) Rosen, M. J. *Surfactants and Interfacial Phenomena*; John Wiley: Hoboken, NJ, 2004.
(11) Stevens, M. M.; George, J. H. Exploring and Engineering the Cell Surface Interface. *Science* **2005**, *310*, 1135−1138.
(12) Koynov, S.; Brandt, M. S.; Stutzmann, M. Black Nonreflecting Silicon Surfaces for Solar Cells. *Appl. Phys. Lett.* **2006**, *88*, 203107.
(13) Bal, J. K.; Hazra, S. Interfacial Role in Room-temperature Diffusion of Au into Si Substrates. *Phys. Rev. B* **2007**, *75*, 205411.
(14) Bal, J. K.; Hazra, S. Time-Evolution Growth of Ag Nanolayers on Differently-Passivated Si(001) Surfaces. *Phys. Rev. B* **2009**, *79*, 155412.
(15) Bal, J. K.; Kundu, S.; Hazra, S. Role of Metal Ions in Growth and Stability of Langmuir-Blodgett Films on Homogeneous and Heterogeneous Surfaces. *Eur. Phys. J. E* **2012**, *35*, 79.
(16) Bansal, A.; Li, X.; Yi, S. I.; Weinberg, W. H.; Lewis, N. S. Spectroscopic Studies of the Modification of Crystalline Si(111) Surfaces with Covalently-Attached Alkyl Chains Using a Chlorination/Alkylation Method. *J. Phys. Chem. B* **2001**, *105*, 10266−10277.
(17) Rivillon, S.; Brewer, R. T.; Chabal, Y. J. Water Reaction with Chlorine-Terminated Silicon (111) and (100) Surfaces. *Appl. Phys. Lett.* **2005**, *87*, 173118.
(18) Webb, L. J.; Michalak, D. J.; Biteen, J. S.; Brunschwig, B. S.; Chan, A. S. Y.; Knapp, D. W.; Meyer, H. M.; Nemanick, E. J.; Traub, M. C.; Lewis, N. S. High-Resolution Soft X-ray Photoelectron Spectroscopic Studies and Scanning Auger Microscopy Studies of the Air Oxidation of Alkylated Silicon(111) Surfaces. *J. Phys. Chem. B* **2006**, *110*, 23450−23459.
(19) Perrine, K. A.; Teplyakov, A. V. Reactivity of Selectively Terminated Single Crystal Silicon Surfaces. *Chem. Soc. Rev.* **2010**, *39*, 3256−3274.
(20) Soria, F. A.; Patrito, E. M.; Paredes-Oliverai, P. On the Mechanism of Silicon Activation by Halogen Atoms. *Langmuir* **2011**, *27*, 2613−2624.
(21) Bal, J. K.; Kundu, S.; Hazra, S. Hydrophobic to Hydrophilic Transition of HF-Treated Si Surface during Langmuir-Blodgett Film Deposition. *Chem. Phys. Lett.* **2010**, *500*, 90−95.
(22) Bal, J. K.; Kundu, S.; Hazra, S. Role of Metal Ions of Langmuir-Blodgett Film in Hydrophobic to Hydrophilic Transition of HF-Treated Si Surface. *Mater. Chem. Phys.* **2012**, *134*, 549−554.
(23) Bal, J. K.; Kundu, S.; Hazra, S. Hydrophilic-like Wettability of Cl-Passivated Ge(001) Surface. *Chem. Phys.* **2012**, *406*, 72−77.
(24) de Gennes, P. G. Wetting: Statics and Dynamics. *Rev. Mod. Phys.* **1985**, *57*, 827−863.
(25) Tadmor, R. Approaches in Wetting Phenomena. *Soft Matter* **2011**, *7*, 1577−1580.
(26) Drelich, J.; Chibowski, E.; Meng, D. D.; Terpilowski, K. Hydrophilic and Superhydrophilic Surfaces and Materials. *Soft Matter* **2011**, *7*, 9804−9828.
(27) Ruan, C. Y.; Lobastov, V. A.; Vigliotti, F.; Chen, S.; Zewail, A. H. Ultrafast Electron Crystallography of Interfacial Water. *Science* **2004**, *304*, 80−84.
(28) Silvestrelli, P. L.; Toigo, F.; Ancilotto, F. Interfacial Water on Cl- and H-Terminated Si(111) Surfaces from First-Principles Calculations. *J. Phys. Chem. B* **2006**, *110*, 12022−12028.
(29) Eves, B. J.; Lopinski, G. P. Formation and Reactivity of High Quality Halogen Terminated Si(111) Surfaces. *Surf. Sci.* **2005**, *579*, L89−L96.
(30) Robinson, I. K.; Tweet, D. J. Surface X-ray Diffraction. *Rep. Prog. Phys.* **1992**, *55*, 599−651.
(31) Daillant, J., Gibaud, A., Eds.; *X-Ray and Neutron Reflectivity: Principles and Applications*; Springer: Paris, 1999.
(32) Gibaud, A.; Hazra, S. X-ray Reflectivity and Diffuse Scattering. *Curr. Sci.* **2000**, *78*, 1467−1477.
(33) Doshi, D. A.; Gibaud, A.; Goletto, V.; Lu, M.; Gerung, H.; Ocko, B.; Han, S. M.; Brinker, C. J. Peering into the Self-Assembly of Surfactant Templated Thin-Film Silica Mesophases. *J. Am. Chem. Soc.* **2003**, *125*, 11646−11655.

(34) Nicole, L.; Boissiere, C.; Grosso, D.; Quach, A.; Sanchez, C. Mesostructured Hybrid Organic Inorganic Thin Films. *J. Mater. Chem.* **2005**, *15*, 3598−3627.
(35) Matheron, M.; Gacoin, T.; Boilot, J.-P. Stabilization of Well-Organized Transient Micellar Phases in CTAB-Templated Silica and Organosilica Thin Films. *Soft Matter* **2007**, *3*, 223−229.
(36) Naudon, A.; Babonneau, D. Characterization of Aggregates in Very Thin Layers by Small-Angle X-ray Scattering Using Grazing Incidence. *Z. Metallkd.* **1997**, *88*, 596−600.
(37) Hazra, S.; Gibaud, A.; Desert, A.; Sella, C.; Naudon, A. Morphology of Nanocermet Thin Films: X-ray Scattering Study. *Physica B* **2000**, *283*, 97−102.
(38) Gibaud, A.; Grosso, D.; Smarsly, B.; Baptiste, A.; Bardeau, J. F.; Babonneau, F.; Doshi, D. A.; Chen, Z.; Brinker, C. J.; Sanchez, C. Evaporation-Controlled Self-Assembly of Silica Surfactant Mesophases. *J. Phys. Chem. B* **2003**, *107*, 6114−6118.
(39) Allen, A. J. Characterization of Ceramics by X-ray and Neutron Small-Angle Scattering. *J. Am. Ceram. Soc.* **2005**, *88*, 1367−1381.
(40) Hazra, S.; Gibaud, A.; Sella, C. Role of Ceramic Matrix and Au-Fraction on the Morphology and Optical Properties of Co-Sputtered Au-Ceramic Thin Films. *J. Appl. Phys.* **2007**, *101*, 113532.
(41) Hazra, S. Morphology and Structure of Gold-Lithium Niobate Thin Film: A Laboratory Source X-ray Scattering Study. *Appl. Surf. Sci.* **2006**, *253*, 2154−2157.
(42) Bal, J. K.; Hazra, S. Atmospheric Pressure Induced Atomic Diffusion into Solid Crystal. *Phys. Rev. B* **2009**, *79*, 155405.
(43) Roth, S. V.; et al. In situ Observation of Cluster Formation during Nanoparticle Solution Casting on a Colloidal Film. *J. Phys.: Condens. Matter* **2011**, *23*, 254208.
(44) Parratt, L. G. Surface Studies of Solids by Total Reflection of X-rays. *Phys. Rev.* **1954**, *95*, 359−369.
(45) Bedzyk, M. J.; Gibson, W.; Golovchenko, J. A. X-ray Standing Wave Analysis for Bromine Chemisorbed on Silicon. *J. Vac. Sci. Technol.* **1982**, *20*, 634−637.
(46) Periodic table of elements: http://www.ptable.com.